Journal of Magnetic Resonance **156,** 313–317 (2002)
doi:10.1006/jmre.2002.2538

COMMUNICATIONS

Cosine Modulated HSQC: A Rapid Determination of $^3J_{HNH\alpha}$ Scalar Couplings in ^{15}N-labeled Proteins

Audrey Petit,* Sébastien J. F. Vincent,† and Catherine Zwahlen*,[1]

*Université de Lausanne, Institut de Chimie Organique/BCH, CH-1015 Lausanne, Switzerland; and †Nestlé Research Center, Vers-chez-les-Blanc, CH-1000 Lausanne 26, Switzerland

Received November 13, 2001; revised March 22, 2002

A two-dimensional HSQC-based NMR method, ^{15}N-COSMO-HSQC, is presented for the rapid determination of homonuclear $^3J_{HNH\alpha}$ couplings in ^{15}N-labeled proteins in solution. Scalar couplings are extracted by comparing the intensity of two separate datasets recorded with and without decoupling of the $^3J_{HNH\alpha}$ during a preparation period. The scalar couplings are introduced through a cosine modulation of the peak intensities. The experiment relies on a BIRD sandwich to selectively invert all amide protons H^N and is very simple to implement. $^3J_{HNH\alpha}$ couplings were determined using both the ^{15}N-COSMO-HSQC and quantitative-*J* on ^{15}N-labeled chemokine RANTES. The two experiments show well-correlated values.

INTRODUCTION

Several different methods are currently available for the measurement of vicinal ^{1}H–^{1}H scalar couplings between amide and alpha protons, $^3J_{HNH\alpha}$. First, three-dimensional experiments requiring ^{13}C,^{15}N-labeled proteins such as E.COSY methods (*1–3*) and DQ/ZQ experiments (*4*). The most widely used method for ^{15}N-labeled proteins is the three-dimensional quantitative-*J* experiment in which the ratio of cross to diagonal peaks is directly related via a tangent function to the scalar coupling (*5–7*). Couplings can also be obtained from multiplet splittings as in *J*-modulated HMQC (*8*) or from two-dimensional spectra in *J*-modulated HSQC (*9*), S^{3}E, and S^{3}CT (*10*) that require a transfer of ^{1}H magnetization via NOESY or TOCSY, *J*-multiplied HSQC (*11*), CT-HMQC-HA/HN (*12, 13*), and CT-HSQC-HA/HN (13). In these last methods, a pair of two-dimensional spectra are recorded with and without selective decoupling of the targeted scalar coupling evolution. The ratio of the cross peaks in these two datasets gives direct access to a cosine function of the $^3J_{HNH\alpha}$ coupling. In the constant-time *J*-modulated HSQC sequence (*13*), selective H^α decouplings of different durations are required which can induce sample heating and can be rather difficult to implement successfully. The ^{15}N-COSMO-HSQC method presented here achieves clean and simple refocusing of all $^3J_{HNH\alpha}$ couplings by a BIRD sandwich (*14, 15*) that selectively inverts all ^{15}N-bound amide protons H^N. In addition, pulsed field gradient sensitivity enhancement (*16*) was included.

[1] To whom correspondence should be addressed at: GeneProt, 2 Rue du Pré-de-la-Fontaine, CH-1217 Meyrin, Switzerland. Fax: +41 22 719 8869. E-mail: catherine.zwahlen@geneprot.com.

RESULTS AND DISCUSSION

Figure 1 shows the pulse sequence of the ^{15}N-COSMO-HSQC experiment. The sequence is composed of an initial period of total duration $2_\tau + 2\delta_1$ during which in-phase ^{1}H coherence is either labeled by a cosine modulation of the $^3J_{HNH\alpha}$ coupling or left unperturbed. After this preparation, a filter followed by sensitivity-enhanced HSQC is applied (*16*). ^{15}N chemical shifts are recorded in the indirect dimension and ^{1}H signal is detected.

After an initial purging of residual ^{15}N magnetization, transverse proton magnetization is excited by a 90°(^{1}H) pulse and let to evolve under the effect of homonuclear couplings leading to a superpositition of in-phase (H_y^N) and antiphase ($2H_x^N H_z^\alpha$) magnetization at point **a** in the sequence. The 180°(^{1}H) proton pulse applied at $\tau/2$ refocuses evolution under the effect of both chemical shifts and ^{1}H–^{15}N heteronuclear scalar couplings during the τ period. A BIRD sandwich (*14, 15*) of duration $2\delta_1 = 1/^1J_{NHN}$ is then applied. At point **a** in the sequence, in-phase coherence H_y^N is converted into longitudinal magnetization H_z^N, while the antiphase term $2H_x^N H_z^\alpha$ is transformed into a superposition of zero- and double-quantum coherence $2H_x^N H_y^\alpha$. For a 180°(^{15}N) pulse, the multiple quantum coherences are modulated by $\cos(\pi\,^1J_{NHN}\,2\delta_1)$, while $^3J_{HNH\alpha}$ homonuclear scalar couplings are effectively decoupled. For a BIRD sandwich delay tuned to $2\delta_1 = 1/^1J_{NHN}$, $\cos(\pi\,^1J_{NHN}2\delta_1) = -1$ and the result is a net inversion of the zero- and double-quantum terms $2H_x^N H_y^\alpha$. On the other hand when a 0°(^{15}N) pulse is applied, the zero- and double-quantum term $2H_x^N H_y^\alpha$ is left unperturbed. The following 90°(^{1}H) pulse converts $2H_x^N H_y^\alpha$ back into antiphase

1090-7807/02 $35.00

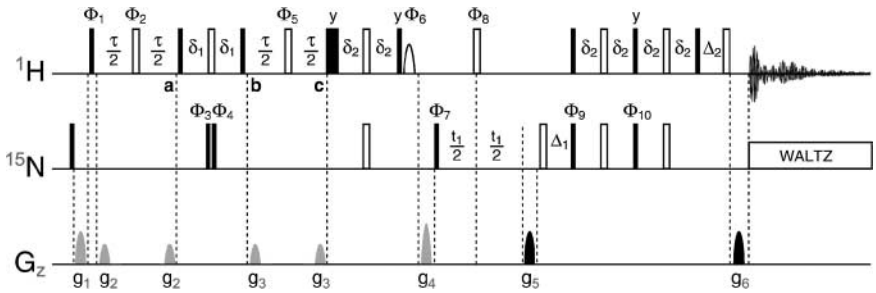

FIG. 1. ^{15}N-COSMO-HSQC pulse sequence for the determination of $^3J_{\mathrm{HNH}\alpha}$ coupling constants in ^{15}N-labeled proteins. Black (white) rectangles are 90° (180°) pulses, the shaped pulse on ^{1}H is a water flip-back 90° pulse of 1.7 ms, and the large black rectangle is a 1-ms purging pulse. The total time for the build-up of cosine modulation is 2τ(40 ms $< 2\tau <$ 60 ms), $2\delta_1 = 1/^1J_{\mathrm{NHN}} = 10.7$ ms is the duration of the BIRD sandwich, $2\delta_2 = 1/(2\,^1J_{\mathrm{NHN}}) = 5.4$ ms is the duration of the INEPT, $\Delta_1 = 1.306$ ms is a compensating delay for optimum phase in t_1 and $\Delta_2 = 1.154$ ms a compensating delay for optimum phase and intensities in t_2. Phase cycling: $\phi_1 = x, -x; \phi_2 = 8(x), 8(-x); \phi_3 = x; \phi_4 = x$ (for 180°(^{15}N)) or $-x$ (for 0°(^{15}N)); $\phi_5 = 16(x), 16(-x); \phi_6 = -x, x; \phi_7 = 2(x), 2(-x); \phi_8 = 4(x), 4(-x); \phi_9 = 4(x), 4(-x); \phi_{10} = 4(y), 4(-y)$ and $\phi_{\mathrm{rec}} = x, -x, -x, x, -x, x, x, -x$. Gradients were either of 500 μs ($g2$ and $g3$) or of 1 ms ($g1$, $g4$, $g5$, and $g6$) and of amplitude in G/cm: $g1 = 22.5$, $g2 = 1.5$, $g3 = 2.5$, $g4 = 35.5$, $g5 = 40$, and $g6 = \pm 4.05$ on alternate t_1-increments for echo–antiecho phase-sensitive acquisition in the indirect dimension.

coherence and the longitudinal term H_z^{N} into transverse single quantum coherence. During the following delay τ, evolution of the coherences happens as for the first τ-period. The purge applied at the end of the delay τ (point **c** in the sequence) prevents the conversion of antiphase magnetization $2H_x^{\mathrm{N}}H_z^{\alpha}$ by the INEPT transfer into a superposition of single- and triple-quantum coherence ($4H_y^{\mathrm{N}}H_x^{\alpha}N_y$). After the sensitivity-enhancement scheme (*16*), those terms would lead to observable magnetization and distort the resulting signals in the ^{15}N-COSMO-HSQC spectra.

As a function of the angle of the ^{15}N pulse located in the middle of the BIRD sandwich, $^3J_{\mathrm{HNH}\alpha}$ couplings are either effectively decoupled (180°(^{15}N) pulse) or evolving for a time 2τ(0°(^{15}N) pulse) leading to a $\cos(\pi\,^3J_{\mathrm{HNH}\alpha}\,2\tau)$ modulation of the spectrum. In proteins, one-bond scalar couplings $^1J_{\mathrm{NHN}}$ are relatively uniform between 91 and 94 Hz and therefore a BIRD sandwich is an efficient way to selectively invert all amide protons with minimal losses.

Neglecting relaxation, the ratio of cross-peak intensity of those two datasets is directly related to the $^3J_{\mathrm{HNH}\alpha}$ coupling constant:

$$\frac{I^{\mathrm{mod}}(\tau)}{I^{\mathrm{dec}}(\tau)} = \cos\left(\pi\,^3J_{\mathrm{HNH}\alpha}2\tau\right). \qquad [1]$$

where I^{mod} is the intensity of a peak in the cosine modulated spectrum obtained by ^{15}N-COSMO-HSQC with a 0°(^{15}N) pulse, and I^{dec} is the intensity of a peak in the decoupled spectrum from a ^{15}N-COSMO-HSQC experiment with a 180°(^{15}N) pulse.

Any differential relaxation mechanisms affecting the signal intensities have to be considered in detail and accounted for. First, relaxation of antiphase terms is known to be affected by the spin-flip rate of the H$^{\alpha}$ and the contribution is nearly linearly proportional to the correlation time τ_{c} (*5, 12*). The antiphase component of magnetization, $2H_x^{\mathrm{N}}H_z^{\alpha}$, will relax faster during the preparation time 2τ than the in-phase magnetization component H_y^{N} by a relaxation rate increased by $T_{1\mathrm{sel}} = 1/\Delta\rho$. In order to describe the evolution of magnetization during the first delay τ, the following equation has to be integrated (*6, 12*),

$$\frac{d}{dt}\begin{pmatrix} i(t) \\ a(t) \end{pmatrix} = \begin{pmatrix} -\rho & \pi J_{\mathrm{true}} \\ -\pi J_{\mathrm{true}} & -(\rho + \Delta\rho) \end{pmatrix}\begin{pmatrix} i(t) \\ a(t) \end{pmatrix}, \qquad [2]$$

where $i(t)$ is the intensity of the in-phase component H_y^{N} relaxing with an auto-relaxation rate ρ, $a(t)$ is the intensity of the antiphase component $2H_x^{\mathrm{N}}H_z^{\alpha}$ relaxing with an auto-relaxation rate $\rho + \Delta\rho$, and J_{true} is the true coupling constant that could be observed if relaxation could be neglected. The analytical solutions to Eq. [2] were given by Ponstingl and Otting (*12*),

$$i(t) = \left[i_0\left(\cos(\pi J_{\mathrm{scaled}}t) + \frac{\eta}{\sqrt{1-\eta^2}}\sin(\pi J_{\mathrm{scaled}}t)\right) + a_0\left(\frac{1}{\sqrt{1-\eta^2}}\sin(\pi J_{\mathrm{scaled}}t)\right)\right]\exp\left\{-\left(\rho + \frac{\Delta\rho}{2}\right)t\right\} \qquad [3]$$

$$a(t) = \left[a_0\left(\cos(2\pi J_{\mathrm{scaled}}t) - \frac{\eta}{\sqrt{1-\eta^2}}\sin(\pi J_{\mathrm{scaled}}t)\right) - i_0\left(\frac{1}{\sqrt{1-\eta^2}}\sin(\pi J_{\mathrm{scaled}}t)\right)\right]\exp\left\{-\left(\rho + \frac{\Delta\rho}{2}\right)t\right\}, \qquad [4]$$

where J_{scaled} is the value of the scalar coupling scaled by $T_{1\mathrm{sel}}$ relaxation according to

$$J_{\mathrm{scaled}} = J_{\mathrm{true}}\sqrt{1-\eta^2} \qquad [5]$$

and η is defined as:

$$\eta = \frac{\Delta\rho}{2\pi J_{\text{true}}}. \quad [6]$$

When the initial conditions are prepared to be $i(0) = -1$ and $a(0) = 0$ at a time $t = \tau$ (point **a** in the sequence), the intensities are given by:

$$i(\tau) = \left[-\cos(\pi J_{\text{scaled}}\tau) - \frac{\eta}{\sqrt{1-\eta^2}}\sin(\pi J_{\text{scaled}}\tau)\right] \times \exp\left\{-\left(\rho + \frac{\Delta\rho}{2}\right)\tau\right\} \quad [7]$$

$$a(\tau) = \frac{1}{\sqrt{1-\eta^2}}\sin(\pi J_{\text{scaled}}\tau)\exp\left\{-\left(\rho + \frac{\Delta\rho}{2}\right)\tau\right\}. \quad [8]$$

The effect of the BIRD sandwich is applied to Eqs. [7] and [8]. Neglecting relaxation during the BIRD sandwich, the 180°(^{15}N) pulse yields

$$a(\tau + 2\delta_1) = -a(\tau), \quad [9]$$

while for the 0°(^{15}N) pulse:

$$a(\tau + 2\delta_1) = a(\tau). \quad [10]$$

Applying Eqs. [3] and [4] with initial condition from point **b** in the sequence given by Eqs. [7] to [10], the final in-phase magnetization at $t = 2\tau$ for a 180°(^{15}N) pulse is given by

$$i(2\tau) = \left[\cos^2(\pi J_{\text{scaled}}\tau) + \frac{1+\eta^2}{1-\eta^2}\sin^2(\pi J_{\text{scaled}}\tau) + \frac{\eta}{\sqrt{1-\eta^2}}\sin(\pi J_{\text{scaled}}2\tau)\right]\exp\left\{-\left(\rho + \frac{\Delta\rho}{2}\right)2\tau\right\} \quad [11]$$

and for a 0°(^{15}N) pulse:

$$i(2\tau) = \left[\cos(\pi J_{\text{scaled}}2\tau) + \frac{\eta}{\sqrt{1-\eta^2}}\sin(\pi J_{\text{scaled}}2\tau)\right] \times \exp\left\{-\left(\rho + \frac{\Delta\rho}{2}\right)2\tau\right\}. \quad [12]$$

An additional relaxation effect needs to be considered: the terms present during the BIRD sandwich duration $2\delta_1$ will experience differential relaxation. The zero- and double-quantum term $2H_x^{\text{N}}H_y^{\alpha}$ will decay with a rate given by $1/T_2^{\text{ZQ/DQ}}$, which is much faster than the $1/T_1$ relaxation rate of the longitudinal term H_z^{N}. This can be described by a factor α defined as:

$$\alpha = \exp\left(\frac{-2\delta_1}{T_2^{\text{ZQ/DQ}}}\right). \quad [13]$$

The antiphase term $a(t)$ will be transformed as

$$a(\tau + 2\delta_1) = \alpha a(\tau), \quad [14]$$

while for the in-phase term

$$i(\tau + 2\delta_1) = i(\tau) \quad [15]$$

since during the BIRD sandwich of duration $2\delta_1$, the longitudinal

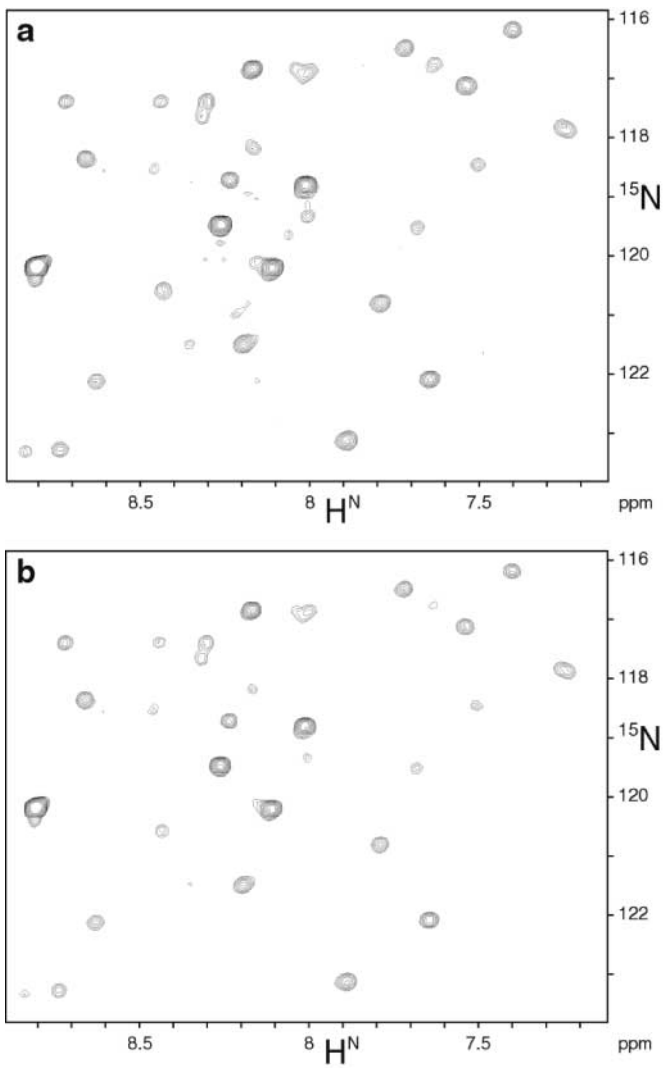

FIG. 2. ^{15}N-COSMO-HSQC spectra with $2\tau = 60$ ms for the determination of $^3J_{\text{HNH}\alpha}$ coupling constants in ^{15}N-labeled RANTES. Eight scans were acquired with 128 complex points in t_1 for a total recording time of 45 min. (**a**) Decoupled spectrum obtained with $\phi_4 = \phi_3$, i.e., applying a 180 (^{15}N) pulse in the middle of the BIRD sandwich. (**b**) Cosine-modulated spectrum obtained with $\phi_4 = -\phi_3$, i.e., applying a 0(^{15}N) pulse in the middle of the BIRD sandwich.

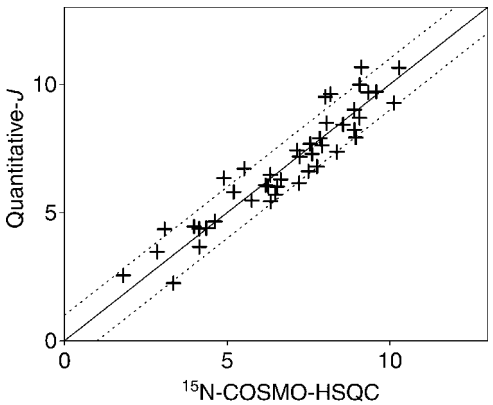

FIG. 3. Comparison of $^3J_{\mathrm{HNH}\alpha}$ coupling constants in ^{15}N-labeled RANTES measured by quantitative-J and ^{15}N-COSMO-HSQC. Dotted line indicates ±1-Hz deviations from ideal correlation.

relaxation of H_z^{N} can safely be neglected. A relaxation time $T_2^{\mathrm{ZQ/DQ}}$ of 20 ms yields a decrease of antiphase magnetization of about 40% for a BIRD sandwich tuned to a $^1J_{\mathrm{NHN}}$ coupling of 92 Hz ($2\delta_1 = 10.9$ ms). Estimation with other $T_2^{\mathrm{ZQ/DQ}}$ times (10 to 30 ms) yield very similar $^3J_{\mathrm{HNH}\alpha}$ coupling constant values and a relaxation time of 20 ms was taken for the fitting and found to be satisfactory for a protein the size of RANTES, i.e., a homodimer of 16 kDa. As a result of the inclusion of relaxation, the magnetization components can be expressed as follows for the 180°(^{15}N) pulse:

$$-i(2\tau) = \left[\cos^2(\pi J_{\mathrm{scaled}}\tau) + \frac{\alpha+\eta^2}{1-\eta^2}\sin^2(\pi J_{\mathrm{scaled}}\tau) + \frac{\eta}{\sqrt{1-\eta^2}}\sin(\pi J_{\mathrm{scaled}}2\tau)\right]\exp\left\{-\left(\rho+\frac{\Delta\rho}{2}\right)2\tau\right\} \quad [16]$$

and for the 0°(^{15}N) pulse:

$$i(2\tau) = \left[\cos^2(\pi J_{\mathrm{scaled}}\tau) - \frac{\alpha-\eta^2}{1-\eta^2}\sin^2(\pi J_{\mathrm{scaled}}\tau) + \frac{\eta}{\sqrt{1-\eta^2}}\sin(\pi J_{\mathrm{scaled}}2\tau)\right]\exp\left\{-\left(\rho+\frac{\Delta\rho}{2}\right)2\tau\right\}. \quad [17]$$

Scalar coupling constants are extracted by taking the ratio of Eqs. [16] and [17],

$$\frac{I^{\mathrm{mod}}}{I^{\mathrm{dec}}} = \frac{\cos^2(\pi J_{\mathrm{scaled}}\tau) - \frac{\alpha-\eta^2}{1-\eta^2}\sin^2(\pi J_{\mathrm{scaled}}\tau) + \frac{\eta}{\sqrt{1-\eta^2}}\sin(\pi J_{\mathrm{scaled}}2\tau)}{\cos^2(\pi J_{\mathrm{scaled}}\tau) + \frac{\alpha+\eta^2}{1-\eta^2}\sin^2(\pi J_{\mathrm{scaled}}\tau) + \frac{\eta}{\sqrt{1-\eta^2}}\sin(\pi J_{\mathrm{scaled}}2\tau)}, \quad [18]$$

where I^{mod} is the intensity measured from the cosine modulated ^{15}N-COSMO-HSQC spectrum recorded with a 0°(^{15}N) pulse in the BIRD sandwich and I^{dec} the intensity measured from the decoupled ^{15}N-COSMO-HSQC spectrum recorded with a 180°(^{15}N) pulse in the BIRD sandwich.

The scalar couplings are directly obtained from Eq. [18] by inserting Eqs. [5], [6], and [13] into Eq. [18], which was used as such to fit the value of J_{true}. $T_{1\mathrm{sel}}$ was set to 100 ms (*5*).

The chemokine RANTES is a carbohydrate binding protein (*17*) involved in recruitement and activation of inflammatory leukocytes via differential attraction of CD4 + T-cells. Its structure was solved by NMR (*18, 19*): the protein is a homodimer at 1-mM concentration with each monomer composed of a three-stranded antiparallel β-sheet in a Greek key motif with the C-terminal α-helix packed across the sheet. $^3J_{\mathrm{HNH}\alpha}$ coupling constants were determined using quantitative-J (*5*) and using the ^{15}N-COSMO-HSQC sequence. The decoupled ^{15}N-COSMO-HSQC spectrum is shown in Fig. 2a, while the cosine-modulatd dataset is shown in Fig. 2b. For most resolved peaks, a value of the $^3J_{\mathrm{HNH}\alpha}$ coupling constant could be obtained both by quantitative-J and by ^{15}N-COSMO-HSQC. Both methods give very similar results. The comparison shown in Fig. 3 indicates that the determination of $^3J_{\mathrm{HNH}\alpha}$ coupling constants using the fitting function of Eq. [18] with one single uniform relaxation

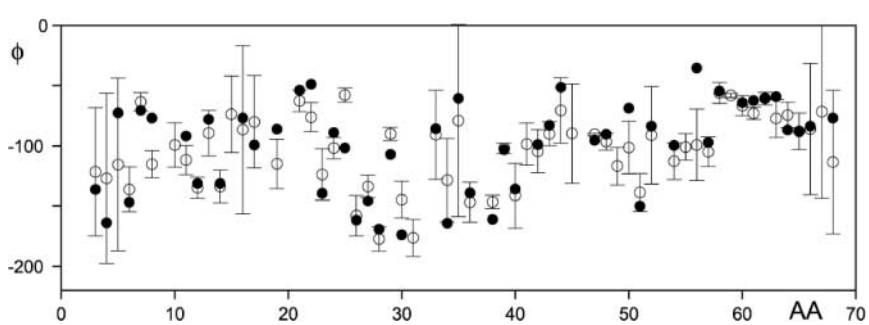

FIG. 4. Comparison of ϕ angles determined from $^3J_{\mathrm{HNH}\alpha}$ coupling constants in ^{15}N-labeled RANTES measured by ^{15}N-COSMO-HSQC (full circles) with the ϕ angles given by the structure published by Skelton *et al.* (*19*), PDB #1rtn (empty circles). The error bars represent one standard deviation of the ϕ angles ($\pm 1\sigma$) as measured in the solution structure.

rate for zero- and double-quantum terms of 20 ms is entirely satisfactory.

The values of the $^3J_{HNH\alpha}$ coupling constants obtained by ^{15}N-COSMO-HSQC yield structural information as can be seen by the comparison of the ϕ angles obtained using the scalar coupling values and the appropriately parametrized Karplus relationship (*5*),

$$J(\phi) = A\cos^2(\phi - 60) + B\cos(\phi - 60) + C, \qquad [19]$$

with $A = 6.51$, $B = -1.76$, and $C = 1.60$ (*5*). Figure 4 shows that coupling values determined by ^{15}N-COSMO-HSQC are consistent with the NMR structure of RANTES by Skelton *et al.* (*19*), at the exception of K25 and K56, both of whose ϕ angles determined by ^{15}N-COSMO-HSQC fit with the angles found in the other NMR structure of RANTES by Chung *et al.* (*18*).

CONCLUSIONS

In this communication, a novel NMR experiment, ^{15}N-COSMO-HSQC, was presented for the measurement of $^3J_{HNH\alpha}$ couplings. The use of a BIRD sandwich for the selective inversion of amide protons allows an efficient homonuclear decoupling scheme whatever the chemical shift range of the amide and α-protons. Also, in contrast to the CT-HSQC-HA/HN sequences using selective H^α decoupling, no complications are expected from nonperfect offset profile and no additional pulse calibrations are requested. The ^{15}N-COSMO-HSQC experiment is highly sensitive and directly applicable to ^{15}N- labeled samples.

ACKNOWLEDGMENTS

CZ acknowledges funding by the Swiss National Fund (FNRS Project 3100-056951.99) and Dr. A. Proudfoot for the sample of ^{15}N-labeled RANTES, while SJFV acknowledges continuous support by Jean-Richard Neeser.

REFERENCES

1. C. Griesinger, O. W. Sørensen, and R. R. Ernst, Two-dimensional correlation of connected NMR transitions, *J. Am. Chem. Soc.* **107,** 6394–6396 (1985).
2. R. Weisemann, H. Rüterjans, H. Schwalbe, J. Schleucher, W. Bermel, and C. Griesinger, Determination of HN,Hα and HN,C' coupling constants in 13C,15N-labeled proteins, *J. Biomol. NMR* **4,** 231–240 (1994).
3. F. Löhr and H. Rüterjans, (H)NCAHA and (H)CANNH experiments for the determination of vicinal coupling constants related to the ϕ-torsion angle, *J. Biomol. NMR* **5,** 25–36 (1995).
4. A. Rexroth, P. Schmidt, S. Szalma, T. Geppert, H. Schwalbe, and C. Griesinger, New principle for the determination of coupling constants that largely suppresses differential relaxation effects, *J. Am. Chem. Soc.* **117,** 10389–10390 (1995).
5. G. W. Vuister and A. Bax, Quantitative *J* correlation: A new approach for measuring homonuclear three-bond *J*(HNHA) coupling constants in ^{15}N-enriched proteins, *J. Am. Chem. Soc.* **115,** 7772–7777 (1993).
6. H. Kuboniwa, S. Grzesiek, F. Delaglio, and A. Bax, Measurement of HN-Ha *J* couplings in calcium free calmodulin using new 2D and 3D water-flipback methods, *J. Biomol. NMR* **4,** 871–878 (1994).
7. F. Löhr, J. M. Schmidt, and H. Rüterjans, Simultaneous Measurement of $^3J_{HN,H^\alpha}$ and $^3J_{H^\alpha,H^\beta}$ coupling constants in ^{13}C,^{15}N-labeled proteins, *J. Am. Chem. Soc.* **121,** 11821–11826 (1999).
8. L. E. Kay and A. Bax, New methods for the measurement of NH-C$^\alpha$H coupling constants in ^{15}N-labeled proteins, *J. Magn. Reson.* **86,** 110–126 (1990).
9. M. Billeter, D. Neri, G. Otting, Y. Q. Qian, and K. Wüthrich, Precise vicinal coupling constants $^3J_{HNH\alpha}$ in proteins from nonlinear fits of *J*-modulated [^{15}N,^{1}H]-COSY experiments, *J. Biomol. NMR* **2,** 257–274 (1992).
10. A. Meissner, T. Schulte-Herbrüggen, and O. W. Sørensen, Spin-state-selective polarization or excitation for simultaneous E.COSY-type measurement of $^3J(C',H\alpha)$ and $^3J(H^N,H\alpha)$ coupling cónstants with enhanced sensitivity and resolution in multidimensional NMR spectroscopy of ^{13}C,^{15}N-labeled proteins, *J. Am. Chem. Soc.* **120,** 3803–3804 (1998).
11. S. Heikkinen, H. Aitio, P. Permi, R. Folmer, K. Lappalainen, and I. Kilpelainen, *J*-multiplied HSQC (MJ-HSQC): A new method for measuring $^3J_{HNH\alpha}$ couplings in ^{15}N-labeled proteins, *J. Magn. Reson.* **137,** 243–246 (1999).
12. H. Ponstingl and G. Otting, Rapid measurement of scalar three-bond ^{1}HN-^{1}Hα spin coupling constants in ^{15}N-labeled proteins, *J. Biomol. NMR* **12,** 319–324 (1998).
13. P. Permi, I. Kilpelainen, A. Annila, and S. Heikkinen, Intensity modulated HSQC and HMQC: two simple methods to measure $^3J_{HNH\alpha}$ in proteins, *J. Biomol. NMR* **16,** 29–37 (2000).
14. J. R. Garbow, D. P. Weitekamp, and A. Pines, Bilinear rotation decoupling of homonuclear scalar interactions, *Chem. Phys. Lett.* **93,** 504–509 (1982).
15. A. Bax, Broadband decoupling in heteronuclear shift correlation NMR spectroscopy, *J. Magn. Reson.* **53,** 517–520 (1983).
16. L. E. Kay, P. Keifer, and T. Saarinen, Pure absorption gradient enhanced heteronuclear single quantum correlation spectroscopy with improved sensitivity, *J. Am. Chem. Soc.* **114,** 10663–10665 (1992).
17. A. E. I. Proudfoot, S. Fritchley, F. Borlat, J. P. Shaw, F. Vilbois, C. Zwahlen, A. Trkola, D. Marchant, P. R. Clapham, and T. N. C. Wells, The BBXB motif of RANTES is the principal site for Heparin binding and controls receptor selectivity, *J. Biol. Chem.* **276,** 10620–10626 (2001).
18. C. Chung, R. M. Cooke, A. E. I. Proudfoot, and T. N. C. Wells, The three-dimensional solution structure of RANTES, *Biochem.* **34,** 9307–9314 (1995).
19. N. J. Skelton, F. Aspiras, J. Ogez, and T. J. Schall, Proton NMR assignment and solution conformation of RANTES, a chemokine of the C-C Type, *Biochem.* **34,** 5329–5342 (1995).